

Wan Muhamad Saridan Wan Hassan, Yusof Munajat and Shamsul Sahibuddin, Physical image quality evaluation of medical radiographs, *Jurnal Fizik Malaysia*, 23, 2002, 201-206.

## **PHYSICAL IMAGE QUALITY EVALUATION OF MEDICAL RADIOGRAPHS**

Wan Muhamad Saridan Wan Hassan<sup>1</sup>, Yusof Munajat<sup>1</sup> & Shamsul Sahibuddin<sup>2</sup>,

<sup>1</sup>Jabatan Fizik, Fakulti Sains, Universiti Teknologi Malaysia,  
81310 Skudai, Johor Darul Ta'zim. Tel: 07-5576160, Fax: 07-5566162, Email:  
saridan@dfiz2.fs.utm.my

<sup>2</sup>Jabatan Sistem dan Kejuruteraan Komputer, Fakulti Sains Komputer dan Sistem  
Maklumat, Universiti Teknologi Malaysia,  
81310 Skudai, Johor Darul Ta'zim.

Key words: diagnostic radiology; medical imaging; modulation transfer function; noise equivalent quanta; noise power spectrum

### **ABSTRACT**

The noise equivalent quanta (NEQ) has been recommended as a measure of physical quality of medical images. Digitised data of medical radiographs in a previous work have been analysed in terms of resolution via the modulation transfer function (MTF) and noise via the noise power spectrum (NPS), but not in terms of NEQ. As the NEQ is currently regarded as a basic device performance measure of the imaging system, it is very useful to be able to determine it. The average gamma of the radiograph was computed, both the MTF and the NPS data were interpolated and these values were used to compute the NEQ. The computation shows that for spatial frequency range 0–0.7 cycles/mm the NEQ of Lanex Regular/T Mat G screen-film combination is slightly lower than that of Lanex Regular/T Mat L, for 0.7–1.5 cycles/mm the NEQ of both are almost the same, and for frequencies greater than 1.5 cycles/mm the NEQ of the former is greater than that of the latter.

## I. INTRODUCTION

For assessing the quality of medical images, the International Commission on Radiation Units and Measurements (ICRU) has recommended the noise equivalent quanta (NEQ) as a measure of the medical imaging device performance [1]. The NEQ combines three specific aspects of performance; the large area transfer characteristics (the gamma), the spatial resolution characteristics (the modulation transfer function (MTF)), and the noise properties (the noise power spectrum (NPS) or the Wiener spectrum) of the imaging device into an overall assessment of performance. In one dimension for small signals limit applicable to the screen-film radiography the NEQ is [2,3]

$$\text{NEQ}(u) = \frac{(\log_{10} e)^2 \gamma^2 \text{MTF}^2(u)}{\text{NPS}(u)} \quad (1)$$

where  $u$  is the spatial frequency in cycles/mm,  $e$  the number 2.71828, and  $\gamma$  the gamma of the film.

NEQ is a measure of the imaging system performance as a photon detector, as it combines the effects of the signal and noise transfer characteristics of the detector to give the apparent number of quanta recorded at a given spatial frequency [3].

In a previous work [4] a substantial amount of digitised data of medical radiographs has been analysed in terms of MTF and NPS, but not in terms of NEQ. As NEQ is currently regarded as a basic device performance measure of the imaging system, it is very useful to be able to determine it. In this work, a PC based software to determine the NEQ is developed using the MTF and NPS data previously collected. The work is expected to contribute towards the general aim of drawing up a physical image quality evaluation protocols.

## II. METHOD AND MATERIALS

### II.A. Measurement set up

The characteristic curve, MTF and NPS data of a few screen-film systems have been collected and calculated as described in a previous study [4]. A summary of data collection and calculation method is now given. Figure 1(a) is the experimental set up for the measurement and Figure 1(b) is the arrangement of the screen-film, bar pattern test object, lead step, and lead mask on the rig when an X-ray exposure is made.

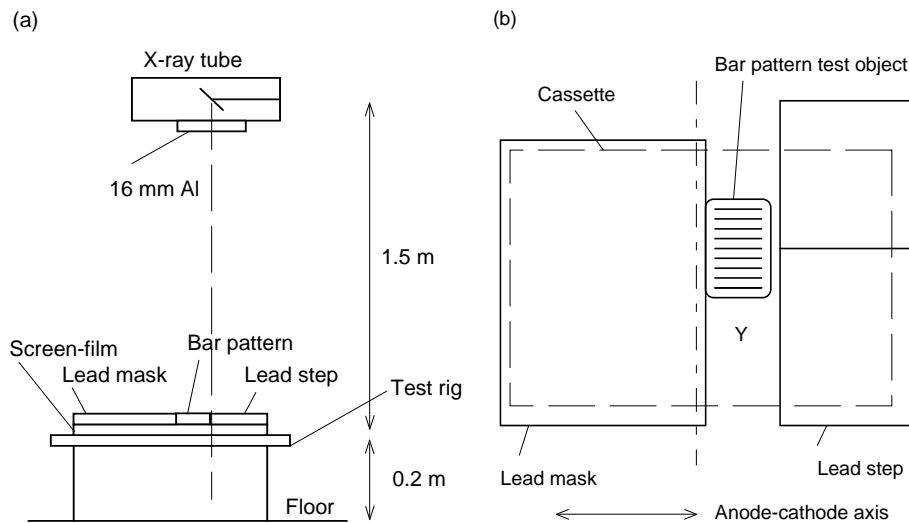


**FIGURE 1.** The experimental set up for the measurement (a), and the arrangement of the screen-film (cassette), bar pattern test object, lead step, and lead mask on the rig when an X-ray exposure is made (b). Image of the bar pattern formed on the radiograph was used to determine the MTF, whilst image of uniform exposure around Y was used to determine the NPS.

The focus-to-film distance was 1.5 m, the same distance used in posteroanterior chest X-ray examination. A long focus-to-film distance helps reduce errors caused by geometric unsharpness and misalignment of the X-ray beam with the test pattern [5]. The distance from the floor to the screen-film was 0.2 m. This helps to reduce back scatter radiation from the floor to the screen-film, as this scatter is expected to be more prominent if the screen-film were placed on the floor.

The light beam diaphragm of the X-ray tube was adjusted so that the beam cone covers a small area approximately the size of the screen-film. A 16 mm thick aluminium filter was attached to the X-ray tube window using PVC tape. This was to simulate the exit beam quality from human body, based on modelling study that the exit radiation at 80 kVp filtered by 15 mm of aluminium is equivalent in quality to the one filtered by 20 cm of water and this is almost tissue equivalent [6,7].

The screen-film was placed on the rig. The bar pattern, the lead step, and the lead mask were then placed on the screen-film, Figure 1(b). The arrangement was intended to minimise the heel effect [8] on the acquired image as the effect was expected to be more pronounced in the anode-cathode axis direction.

The square wave test object was Type 53 PTW-Freiburg bar pattern (available from Facility for the Assessment of X-ray Imaging at Leeds University, The General Infirmary, Leeds) with 19 groups of line pairs of 0.05 mm lead thickness. Each line pair group has four and a half line pairs, except the first which has two. The groups are 0.25, 0.5, 0.6, 0.7, 0.85, 1.0, 1.2, 1.4, 1.7, 2.0, 2.4, 2.9, 3.5, 4.2, 5.0, 6.0, 7.0, 8.5, and 10 line pairs/mm.

The lead step was used for another MTF determination not covered by this article [4].

The lead mask was a 2 mm thick lead sheet. It masked half of the screen-film from being exposed to the X-ray. This half can later be used for making another exposure.

To expose the unmasked region of the screen-film, the rig was positioned so that the region was in the primary X-ray beam axis. The region was exposed using exposure factor of 80 kVp, 2 mAs. The image of the bar pattern will be used for the determination of the MTF, whilst the image of uniform X-ray radiation will be used for the determination of NPS (region Y, Figure 1(b)).

Another exposure was made at the mAs value of 2.4 using the previously masked region of the screen-film. This way two exposures per film were collected. The film was developed, and optical densities of the two background regions of this film were measured using a portable densitometer (X-OGRAPH Digit-X Densitometer, Appleford Instrument Limited, Abingdon, Oxfordshire, UK). Based on the two optical density values, more exposures were made on other films using mAs values of 1, 1.2, 1.3, 1.5, 1.6, and 2.6. To measure the X-ray exposure or dose, the rig was removed, and an ion chamber was placed at the same level as the screen-film. The doses for all the different exposure factors used were then measured. The ion chamber model 90X6 and the radiation monitor controller model 9010 (Radcal Corporation, Monrovia, California, USA) were used for the purpose. Relative exposure values were computed from this measurement.

The characteristic curve of the screen-film (from which the gamma can be computed) was obtained from optical density and dose measurements. The optical densities of uniformly exposed regions of the films were again measured with a transmission densitometer (model DT 1405, PARRY, Newbury, Berkshire, UK) which was calibrated to a national standard, for a more accurate optical density measurement. The optical density and relative exposure data were fitted by a computer program and a fitted data file of optical density versus relative exposure was produced. This file was used for the linearisation or conversion of optical density to exposure values. Figure 2 shows the characteristic curve for this work.

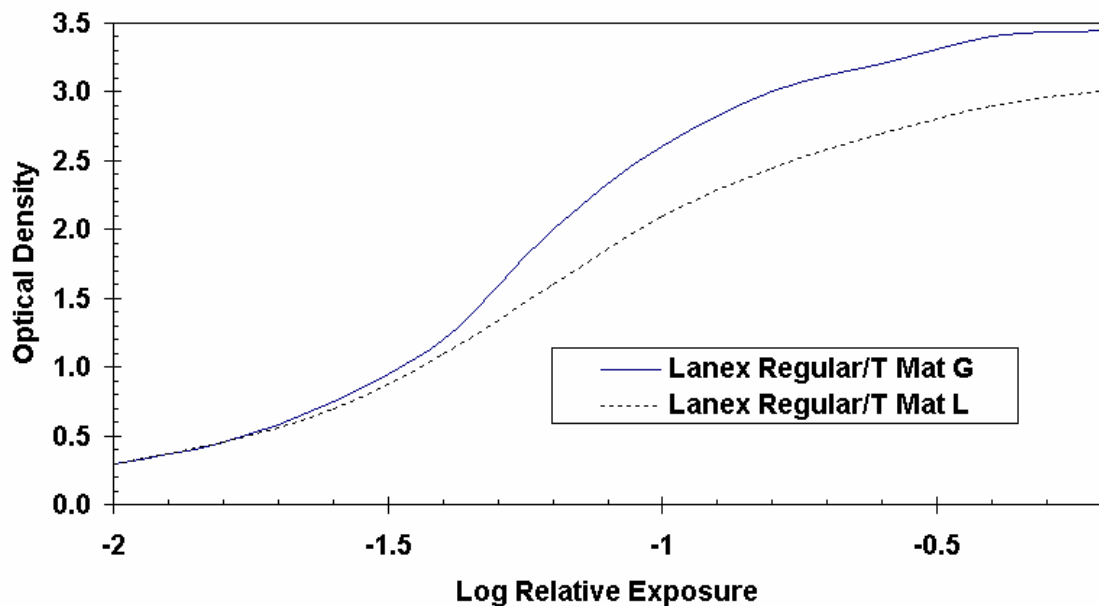


**FIGURE 2.** The characteristic curve of the screen-films used in the work.

## II.B. Film scanning

The image of the bar pattern was scanned by a microdensitometer (Photoscan System P-1000, Optronics International Inc., Chelmsford, Massachusetts, USA). It is a rotating drum device, and collects data in a two dimension image with pixel size of  $12.5 \mu\text{m}$  square. The sampling interval was  $12.5 \mu\text{m}$ . The data are in the form of digital pixel values 0–255 (8-bit) which correspond to 0–3 optical density units. The scanning aperture, which was imaged through a 10 $\times$ , numerical aperture of 0.25 objective, and a 10 $\times$  eyepiece lens, has dimensions of  $12.5 \times 12.5 \mu\text{m}^2$  at the film plane.

The microdensitometer was interfaced to and controlled by a personal computer (ELONEX PC-466/VL, 486DX2 processor at 66 MHz, Elonex Plc., Apsley Way, London, UK). At the end of each scan, a binary image file with 512 bytes header was written on the hard disk.

## II.C. MTF calculation

For the MTF calculation, the scan size was 6000 pixels by 100 pixels; this corresponds to an area of 75 mm by 1.25 mm on the film. This means the scan consists of 100 traces of adjacent scans each of 6000 pixels long.

Data were converted to diffuse density by way of a calibrated sensitometric strip consisting of 21 optical density steps. Diffuse optical densities of the steps were measured by the transmission densitometer. The sensitometric strip was then scanned

by the microdensitometer. The average pixel value for each of the 21 steps of the sensitometric strip was calculated by a computer program, and this value was matched with the corresponding measured diffuse density. This way values of diffuse optical density versus average pixel values which make up the microdensitometer calibration graph was obtained. Figure 3 shows the microdensitometer calibration curve for this work. Density values were then converted to relative exposure values by means of the screen-film characteristic curve.

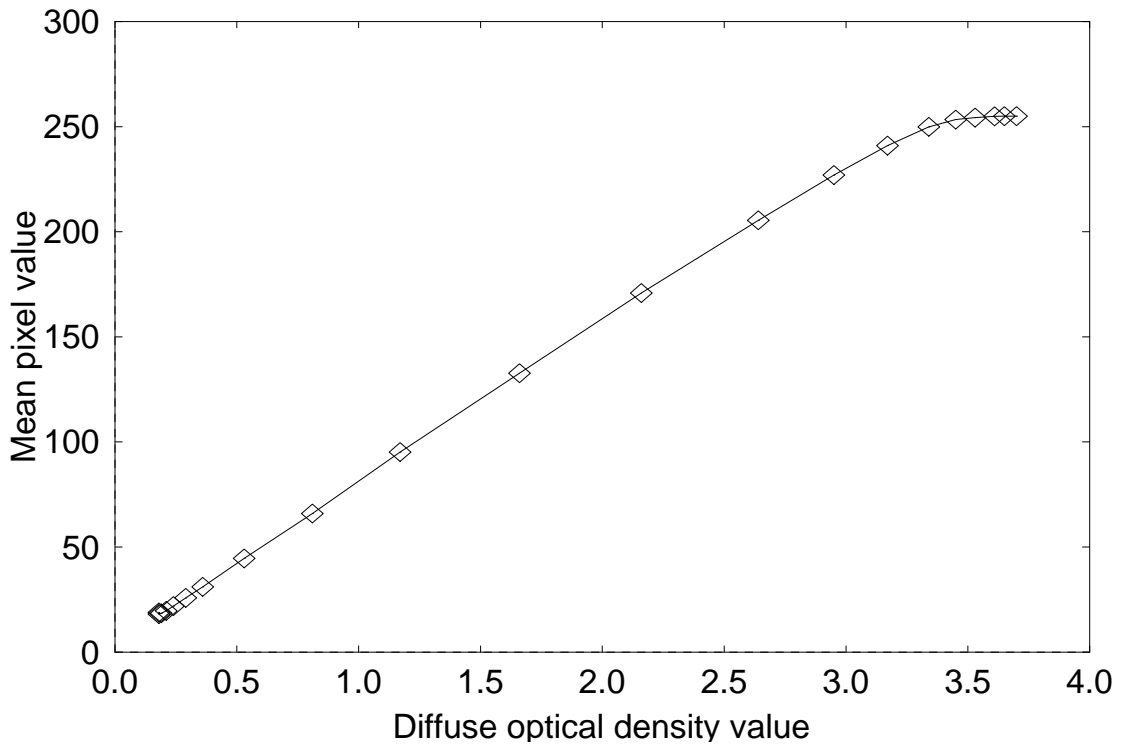


**FIGURE 3.** The microdensitometer calibration curve used in the work.

A computer program was used to calculate the MTF. The program displays the bar pattern image on the screen, and a rectangular region of interest could be selected by a mouse. The program then calculates the maximum and minimum of each frequency group. For example if a region of interest, say of 5000 pixels by 90 pixels was selected, then the adjacent pixel values were added and averaged width wise, i.e., average pixel value of 90 traces. These average pixel values were converted to diffuse density values and then to relative exposure values. Then the maximum and minimum of the modulation of each frequency group were determined, and a text file containing this information was written. This in effect is the average peak and trough values for the response to the square wave pattern. Next the square wave response factors for each frequency group,  $r(u)$ , calculated by

$$r(u) = \frac{\Phi_{max} - \Phi_{min}}{\Phi_{max} + \Phi_{min}} \quad (2)$$

where  $\Phi_{max}$  and  $\Phi_{min}$  are the peak and trough values in relative exposure units respectively, and  $u$  the spatial frequency in line pairs/mm mention in section II.A. The factors were normalised by dividing the factors by the square wave response factor value at 0.25 line pair/mm. This 0.25 line pair/mm was the lowest grating line pairs size on Type 53 bar pattern. The modulation transfer factors,  $MTF(u)$ , were then calculated using the square wave response factors by the formula [10]:

$$MTF(u) = \frac{\pi}{4} \left[ r(u) + \frac{r(3u)}{3} - \frac{r(5u)}{5} + \frac{r(7u)}{7} + \frac{r(11u)}{11} - \frac{r(13u)}{13} - \frac{r(15u)}{15} - \frac{r(17u)}{17} - \frac{r(19u)}{19} - B_k \frac{r(ku)}{k} \dots \right] \quad (3)$$

where  $k$  takes on the odd values 1, 3, 5, etc., and  $B_k$  is 1, 0, or -1 according to the formulae

$$\begin{aligned} B_k &= (-1)^m (-1)^{(k-1)/2} & \text{if } & p = m, \\ B_k &= 0 & \text{if } & p < m. \end{aligned}$$

and  $m$  is the total number of primes into which  $k$  can be factored, and  $p$  is the number of different prime factors in  $k$ . These values were then normalised by the value of the factor at 0.25 line pair/mm to get the final MTF. Figure 4 shows the MTF of Lanex Regular/T Mat G and Lanex Regular/T Mat L obtained. The MTF values are available only at discrete spatial frequencies values of 0.25, 0.5, 0.6, 0.7, 0.85, 1.0, 1.2, 1.4, 1.7, 2.0, 2.4, 2.9, 3.5, 4.2 cycles/mm for Lanex Regular/T Mat G, and at 0.25, 0.5, 0.6, 0.7, 0.85, 1.0, 1.2, 1.4, 1.7, 2.0, 2.4, 2.9 cycles/mm for Lanex Regular/T Mat L, corresponding to the line pair groups available on the bar pattern.

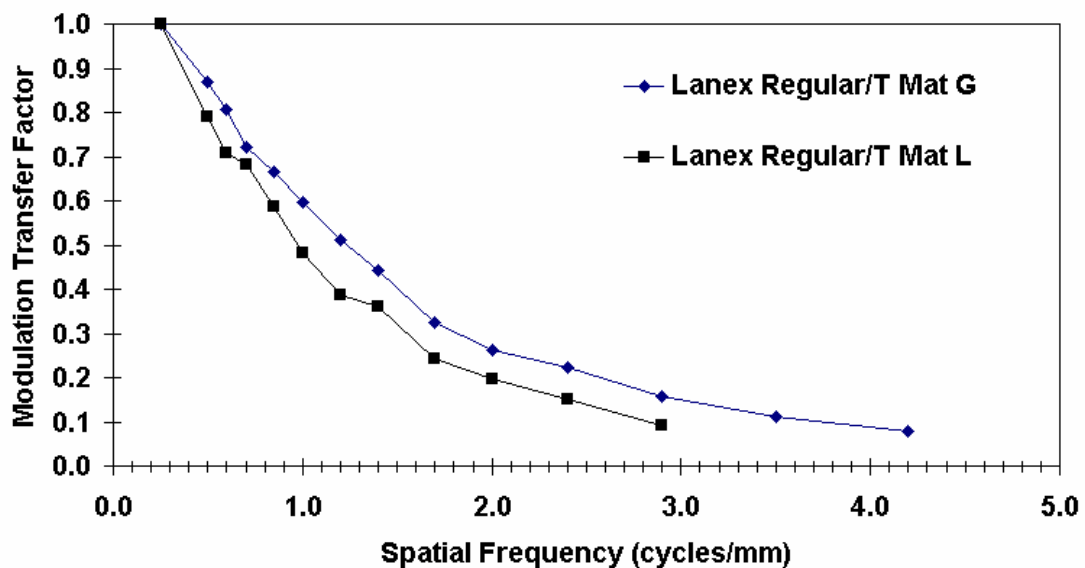


**FIGURE 4.** The MTF of Lanex Regular/T Mat G and Lanex Regular/T Mat L obtained using the square wave response function method.

#### II.D. NPS calculation

The same film was used for the NPS determination. The uniform background region of the film, around Y in Figure 1(b), was scanned by the microdensitometer. The size of the scan was usually 6000 pixels by 300 pixels which correspond to a physical area of 75 mm by 3.75 mm. The image matrix was then subjected to the NPS calculation.

The NPS calculation using the fast digital Fourier transform method has been described elsewhere [11], and the summary of which is now given. The pixel values of the image data were converted to the optical density values by means of the microdensitometer calibration curve. Then the optical density fluctuation values about the mean density were obtained by subtracting the mean density from the density values. The data were low-pass-filtered by averaging pairs of pixels, followed by low-frequency filtering to eliminate very low-frequency components. A slit trace was synthesised by averaging adjacent traces and the trace was segmented to segments of 256 data points per segment with overlap of 128 data points. Data in each segment were windowed and fast Fourier transformed. The Fourier coefficients were squared and normalised to obtain the noise power spectrum.

Figure 5 shows the NPS of Lanex Regular/T Mat G and Lanex Regular/T Mat L obtained using the method. The NPS values are at spatial frequencies 0, 0.3125, 0.6250, 0.9375, 1.2500, 1.5625, ..., 10.0 cycles/mm. These spatial frequencies are multiples of the frequency interval 0.3125 cycles/mm. The frequency interval is the reciprocal of the product of the length of fast Fourier transform (256) and the sampling interval ( $12.5\mu\text{m} = 0.0125\text{ mm}$ ), see [11] for the details. Thus the spatial



frequencies at which the NPS values are available are different from the spatial frequencies at which the MTF values are available.

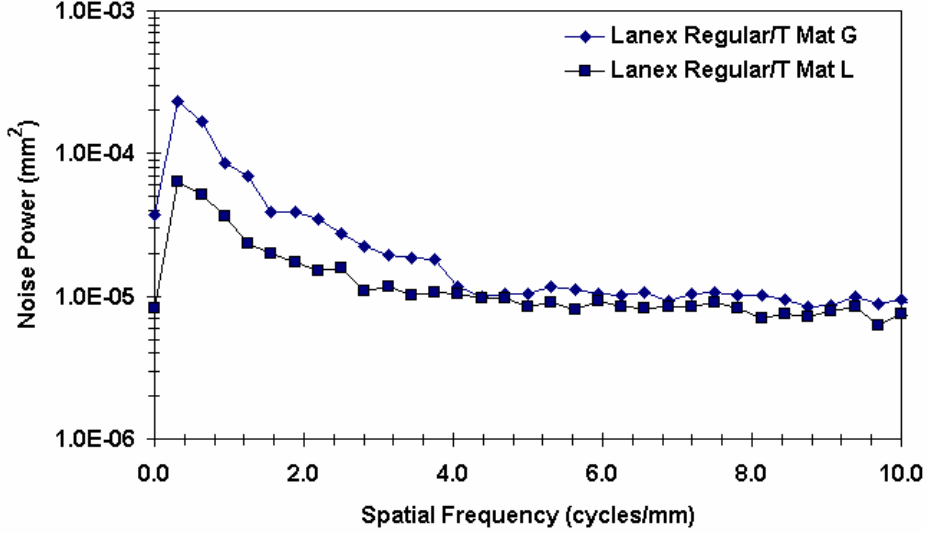


**FIGURE 5.** The NPS of Lanex Regular/T Mat G and Lanex Regular/T Mat L obtained using the fast digital Fourier transform method.

## II.E. NEQ computation

The NEQ was computed using Equation (1) by writing several MATLAB “.m” files. First, the average gamma was computed from the characteristic curve of the screen-films using the definition [12]

$$\gamma = \frac{D_2 - D_1}{\log_{10} X_2 - \log_{10} X_1} \quad (4)$$

where  $X_1$  and  $X_2$  are exposures that give net optical density of  $D_1 = 1.0$  and  $D_2 = 2.0$  above base plus fog level respectively.

As the MTF data available were at spatial frequency 0.25, 0.5, 0.6, 0.7, 0.85, 1.0, 1.2, 1.4, 1.7, 2.0, 2.4, 2.9, 3.5, 4.2 cycles/mm for Lanex Regular/T Mat G, and at 0.25, 0.5, 0.6, 0.7, 0.85, 1.0, 1.2, 1.4, 1.7, 2.0, 2.4, 2.9 cycles/mm for Lanex Regular/T Mat L, linear interpolation was performed at spatial frequency 0, 0.1, 0.2, 0.3, ..., 4.2 cycles/mm for Lanex Regular/T Mat G, and at spatial frequency 0, 0.1, 0.2, 0.3, ..., 2.9 cycles/mm for Lanex Regular/T Mat L, respectively. The MTF value at 0 cycle/mm was assigned as 1. Similarly, the NPS data available at spatial frequency 0, 0.3125, 0.6250, 0.9375, ..., 10.0 cycles/mm were linearly interpolated at spatial frequencies 0, 0.1, 0.2, 0.3, ..., 10.0 cycles/mm. This way both the MTF and NPS values at spatial frequency interval of 0.1 cycle/mm ready for further computation.

Finally, the NEQ was computed as per Equation (1), using the average gamma, the interpolated MTF, and the interpolated NPS values. Thus the computation gave the NEQ at spatial frequency 0, 0.1, 0.2, 0.3, ... , 4.2 cycles/mm for Lanex Regular/T Mat G, and at spatial frequency 0, 0.1, 0.2, 0.3, ... , 2.9 cycles/mm for Lanex Regular/T Mat L, respectively.

### **III. RESULTS AND DISCUSSION**

The NEQs computed by the MATLAB codes are shown in Figure 4. For spatial frequency range 0–0.7 cycles/mm, the NEQ of Lanex Regular/T Mat G (LR/TMG) is slightly lower than that of Lanex Regular/T Mat L (LR/TML); for frequency range 0.7–1.5 cycles/mm, the NEQs of both are almost the same; and for frequencies greater than 1.5 cycles/mm, the NEQ of the former is higher than that of the latter. This suggests that a signal with low frequency content (0-0.7 cycles/mm) shows better on LR/TML, but a signal with high frequency content (higher than 1.5 cycles/mm) shows better on LR/TMG.

The NEQs of both screen-film systems obtained by manual calculation are also shown in the figure. Here the MTFs have been fitted to an analytical curve and extrapolated, thus the calculation provides NEQ values for larger frequency ranges. The results of the calculation and the computation agree very well.

For comparison the NEQs of DuPont Cronex Detail/XRP, Par Speed/XRP, and Hi-Plus/XRP reported in reference [3], and Quanta Fast Detail/C10S reported in reference [13] are also shown in the figure. Our computed results are smaller than those compared, but the order of magnitude of the NEQ values are the same. This might be due to lower MTF values available for the computation.

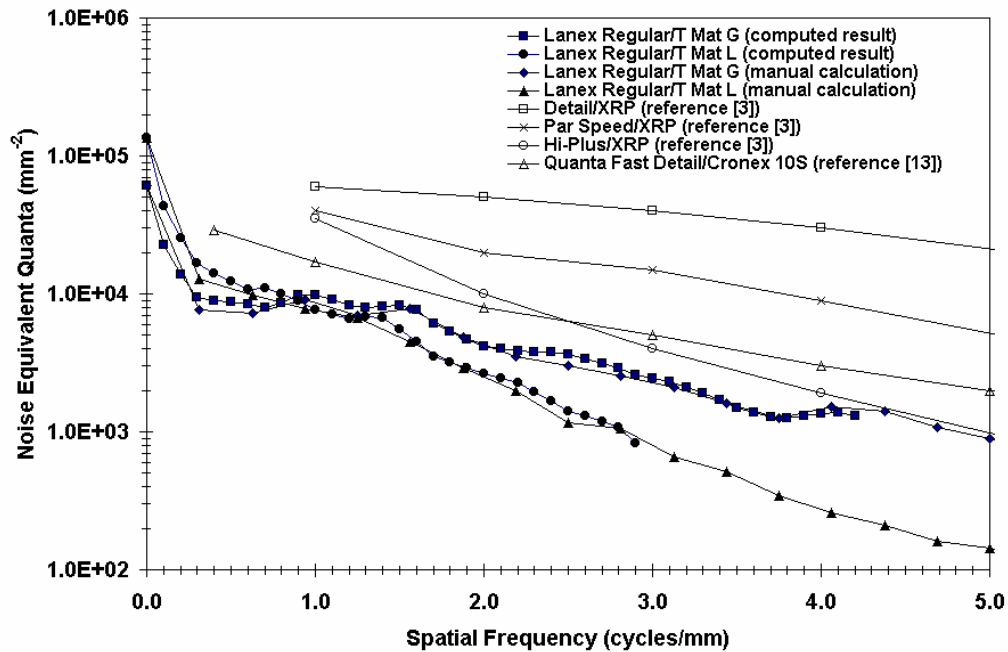


**FIGURE 4.** The NEQs of Lanex Regular/T Mat G and Lanex Regular/T Mat L obtained by the computation and by manual calculation. Also shown are the NEQs of DuPont Cronex Detail/XRP, Par Speed/XRP, and Hi-Plus/XRP reported in reference [3], and Quanta Fast Detail/C10S reported in reference [13].

#### IV. CONCLUSION

A physical image quality measure, the noise equivalent quanta (NEQ), was computed using MATLAB codes given the characteristic curve, modulation transfer function and noise power spectrum data of medical radiographs. The NEQs of Lanex Regular/T Mat G and Lanex Regular/T Mat L were computed; for spatial frequency range 0–0.7 cycles/mm the NEQ of Lanex Regular/T Mat G screen-film combination is slightly lower than that of Lanex Regular/T Mat L; for frequency range 0.7–1.5 cycles/mm, the NEQs of both are almost the same; and for frequencies greater than 1.5 cycles/mm the NEQ of the former is greater than that of the latter. The developed codes should be useful for diagnostic screen-film imaging, but might also be applicable for other imaging modalities because the general nature of the NEQ concept.

#### ACKNOWLEDGEMENT

This work was supported in part by the Research Management Centre, Universiti Teknologi Malaysia, grant number 71761.

## REFERENCES

- [1] ICRU, Medical Imaging – The Assessment of Image Quality, ICRU Report 54, International Commission on Radiation Units and Measurements, Bethesda, Maryland, USA (1995).
- [2] C. E. Metz, R. F. Wagner, K. Doi, D. G. Brown, R. M. Nishikawa, and K. J. Myers, Toward consensus on quantitative assessment of medical imaging systems, *Medical Physics*, **22**, 1057–1061 (1995).
- [3] J. M. Sandrik and R. F. Wagner, Absolute measures of physical image quality: Measurement and application to radiographic magnification, *Medical Physics*, **9**, 540–549 (1982).
- [4] W. M. S. W. Hassan, Measurement of modulation transfer function and Wiener spectrum of diagnostic X-ray screen-film systems in a hospital setting, Ph.D. thesis, University of Aberdeen (1998).
- [5] J. Morishita, K. Doi, R. Bollen, P. C. Bunch, D. Hoeschen, G. Sirand-rey and Y. Sukenobu, Comparison of two methods for accurate measurement of modulation transfer functions of screen-film systems, *Medical Physics*, **22**, 193–200 (1995).
- [6] FAXIL, Tutorial on the image quality characteristics of radiographic screen-film systems and their measurement, MDD Evaluation Report MDD/94/34, Facility for the Assessment of X-ray Imaging at Leeds University, The General Infirmary, Leeds (1994).
- [7] H. M. Kramer, Radiation qualities for tests in diagnostic radiology, *Radiation Protection Dosimetry*, **43**, 107–110 (1992).
- [8] H. E. Johns and J. R. Cunningham, *The Physics of Radiology*, 4th. ed., Charles C. Thomas Publisher, Springfield, Illinois, USA (1983), pp. 66–68.
- [9] K. Doi, Y. Kodera, L. N. Loo, H. P. Chan, Y. Higashida, and R. J. Jennings, MTF's and Wiener spectra of radiographic screen-film systems – Volume II (Including speeds of screens, films, and screen-film systems), HHS Publication FDA 86-8257, U.S. Department of Health and Human Services, Public Health Service, Food and Drug Administration, Center for Devices and Radiological Health, Rockville, Maryland (1986).
- [10] J. W. Coltman, The specification of imaging properties by response to a sine wave input, *Journal of the Optical Society of America*, **44**, 468–471 (1954).
- [11] W. M. S. W. Hassan, Measurement of Wiener spectrum of radiographic screen-film systems, *Jurnal Teknologi*, **34(C)**, 35-42 (2001).
- [12] H. E. Johns and J. R. Cunningham, *The Physics of Radiology*, 4th. ed., Charles C. Thomas Publisher, Springfield, Illinois, USA (1983), p. 580.
- [13] FAXIL, Physical evaluation of the imaging performance of Dupont ultra-vision screen-film system, MDA Evaluation Report MDA/94/40, Facility for the Assessment of X-ray Imaging at Leeds University, The General Infirmary, Leeds (1994).